

## ExpeER

# Distributed Infrastructure for EXPERimentation in Ecosystem Research

Grant Agreement Number: 262060

**SEVENTH FRAMEWORK PROGRAMME**  
**Capacities**  
**Integrating activities: Networks of Research Infrastructures (RIs)**  
**Theme: Environment and Earth Sciences**

### DELIVERABLE D8.3

Deliverable title: Report on performance tests of pilots

**Abstract:** This report provides the performance test results of pilot experiments in which (a) improved algorithms and systems for climate simulation are applied, (b) alternative designs for studying biodiversity-vulnerability relationships under environmental change are used.

Due date of deliverable: M36

Actual submission date: M54

Start date of the project: December 1<sup>st</sup>, 2010

Duration: 54 months

Organisation name of lead contractor: CNR

Contributors: CNR, UA

Revision N°: Final

Dissemination level:

<b>PU</b> Public (must be available on the website)	<b>X</b>
<b>PP</b> Restricted to other programme participants (including the Commission Services)	
<b>RE</b> Restricted to a group specified by the consortium (including the Commission Services) (precise to whom it should be addressed)	
<b>CO</b> Confidential, only for members of the consortium (including the Commission Services)	

## Table of Content

<b>1.</b>	<b>EXECUTIVE SUMMARY</b>	<b>1</b>
<b>2.</b>	<b>TASK T8.1: DESIGNING REALISTIC WARMING EXPERIMENTS</b>	<b>2</b>
2.1	RATIONALE	2
2.2	PROCEDURE AND FORMULAS	2
2.3	IMPLEMENTATION	5
<b>3.</b>	<b>TASK T8.2: USING COMPUTATIONAL FLUID DYNAMICS (CFD) TO DESIGN CO<sub>2</sub> ENRICHMENT TECHNOLOGIES</b>	<b>6</b>
3.1	THE FACE TECHNOLOGY: PAST, PRESENT AND FUTURE	6
3.2	AN INNOVATIVE FACE DESIGN	8
3.3	CONTROL ALGORITHM AND NEW HARDWARE TESTS	8
3.4	CONCLUSION	11
<b>4.</b>	<b>TASK T8.4: NEW GENERATION BIODIVERSITY/CLIMATE CHANGE EXPERIMENTS</b>	<b>13</b>
4.1	ASSESSING BIODIVERSITY - ECOSYSTEM FUNCTIONING RELATIONSHIPS IN NATURAL SYSTEMS	13
4.1.1	RATIONALE	13
4.1.2	EXPERIMENTAL DESIGN	13
4.1.3	RESULTS AND CONCLUSION	14
4.2	QUICK METHOD FOR CHARACTERIZING SPECIES INTERACTIONS IN A PLANT COMMUNITY	16
4.2.1	RATIONALE	16
4.2.2	EXPERIMENTAL DESIGN	16
4.2.3	RESULTS AND CONCLUSION	17
	<b>ANNEX</b>	<b>19</b>

## 1. Executive summary

---

In this report we describe performance tests of pilot experiments in which improved algorithms and systems for climate simulation are applied, and performance tests of pilot experiments in which alternative designs for studying biodiversity-vulnerability relationships are applied. Performance tests of new types of model ecosystems and small-scale proxies of whole ecosystems in ecology were already described in deliverable D8.1. The pilots where improved algorithms and systems for climate change simulation were applied, were twofold. One experiment explored an novel and advanced technique to administer infrared heating to plant communities in free air conditions in the field in order to better simulate climate warming or heatwaves. This test proved successful. The other pilot on climate change tested novel algorithms for enhancing the atmospheric CO<sub>2</sub> concentration in free air conditions in the field. In a computer simulation with one of these algorithms, it was demonstrated that stable CO<sub>2</sub> gradients can be produced in which vegetation can be exposed to a range of CO<sub>2</sub> concentrations at the same time, which is a major advance relative to classical FACE systems. The pilot experiments in which alternative designs for studying biodiversity-vulnerability relationships were applied, were also twofold. One performance test focused on using the natural small-scale spatial variation in species richness in the field to study diversity - ecosystem functioning relationships. This test did not prove to be sufficiently robust and was not continued. A second performance test focused on easy and rapid detection species interactions in the field, in order to better explain diversity - ecosystem functioning relationships. This test proved successful. Limitations and opportunities to apply this new method are discussed.

## 2. Task T8.1: Designing realistic warming experiments

---

### Field warming experiments with infrared irradiation: control methods to apply infrared irradiation

(contribution by UA)

#### 2.1 Rationale

Using infrared heating in free-air conditions has a number of important advantages, among which are chief the relatively natural micro-meteorological conditions (wind speed, humidity, insolation, etc.). The control used to administer the infrared heating load is obviously very important. Infrared heating warms the surface directly, not the air, while meteorological and climatological data and scenarios consider air temperatures instead of canopy temperatures. This makes it more difficult to set the level of (canopy) warming, as the relationship between air and canopy temperatures is not linear or constant. The latter are not only affected by meteorological conditions, but also by the characteristics and responses of the plants: leaf size, angle, roughness, etc., but also responsiveness of stomates to drying.

Many current control methods for infrared heating maintain a constant temperature difference between warmed and control plots. This also implies that any responses of the vegetation to conditions that differ in the warmed plots are filtered out. Drought causing higher leaf temperatures when stomatal conductance decreases in response to drier conditions is for example not possible if canopy temperatures are increased by a fixed amount. An alternative method is to increase the radiation input by a fixed amount (e.g.  $1000 \text{ W m}^{-2}$ ), so that canopy temperatures can still vary because of plant responses. Unfortunately, this method is uncontrolled, meaning that no target temperature can be set. An improved method (De Boeck & Nijs 2011) should reconcile the controllability of the constant temperature increase approach and the tolerance for plant feedbacks of the constant radiation flux approach.

#### 2.2 Procedure and formulas

We propose a new control method based on energy balance calculations. The general principle of this method was already briefly outlined in deliverable D8.2, and here we present the complete and detailed protocol as well as test in the field. The control method works in three steps. First, the canopy conductance of the (unheated) reference plot has to be determined. Secondly, a theoretical canopy temperature associated with given (target) air temperature needs to be calculated. Finally, the energy output of the infrared heaters required to achieve said theoretical canopy temperature has to be computed. The formulas are given here in full:

Step 1:

$$g_v = \frac{-p_a [(T_{canopy} - T_a) c_p (g_r + g_{Ha}) - R_{abs} + \varepsilon_s \sigma T_a^4 + G]}{\lambda D + p_a (T_{canopy} - T_a) \lambda s}$$

Step 2:

$$T_{canopy} = (T_a + o) + \frac{R_{abs} - \varepsilon_s \sigma (T_a + o)^4 - G - \frac{\lambda g_v D}{p_a}}{c_p (g_r + g_{Ha}) + \lambda s g_v}$$

Step 3:

$$R_{abs} = [(g_{Ha} + g_r) \cdot c_p + \lambda s g_v] \cdot (T_{canopy} - T_a) + \varepsilon_s \sigma T_a^4 + G + \frac{\lambda g_v D}{p_a}$$

(and increase infrared heater output until measured  $R_{abs}$  = calculated  $R_{abs}$ )

The following parameters are continuously measured (automated):

$R_{abs}$  = difference between incoming radiation and reflected radiation

$T_a$  = air temperature (control plot)

$T_{canopy}$  = canopy temperature (control plot)

$G$  = soil heat flux (value from heat flux plate in control)

$RH$  = relative humidity of the control plot

$p_a$  = atmospheric pressure

$u(z)$  = wind speed at height  $z$  ( $m s^{-1}$ )

The following parameters require manual input:

$z$  = measuring height (m)

$h$  = vegetation height (input every few days to take growth into account), and  $z > h$

$o$  = offset for  $T_a$  (input each day based on weather predictions, this allows implementing exact  $T_{air}$  scenarios)

These are constants:

$\varepsilon_s$  = the surface emissivity = 0.97

$\sigma$  = the Stefan–Boltzman constant =  $5.670 \times 10^{-8} W m^{-2} K^{-4}$

$c_p$  = the specific heat of air =  $29.3 J mol^{-1} K^{-1}$

$g = 9.81 m s^{-2}$

Other inputs are calculated:

$\lambda$  = the latent heat of vapourisation for water =  $-42.575 T_a + 44994$  (kJ mol<sup>-1</sup>)

$g_r$  = the radiative conductance =  $4 \varepsilon_s \sigma T_a^3 / c_p$

$$e_s(T) = 0.611 e^{\frac{17.502 T_a}{T_a + 240.97}}$$

$D$  = the vapour deficit of the air =  $(1 - RH) * e_s(T)$  (in Pa)

$$\Delta = 17.502 * 240.97 * e_s(T) / (240.97 + T_a)^2$$

$s$  = the slope of the saturation mole fraction =  $\Delta / p_a$

$$\rho = 44.6 \frac{p_a}{101.3} \frac{273.15}{T_a} \quad (\text{molar density of air}) \quad (T \text{ in Kelvin})$$

$d$  = zero plane displacement height (m) =  $0.65 * h$

$Z_M$  = momentum roughness length =  $0.1 * h$

$Z_H$  = heat roughness length =  $0.2 * Z_M$

Finally, iterative calculation is required:

\*For unstable (i.e.  $T_a < T_{\text{canopy}}$ ) flow:

$$\psi_H = -2 \ln \left[ \frac{1 + (1 - 16\zeta)^{0.5}}{2} \right]$$

$$\psi_M = 0.6 \psi_H$$

\*For stable (i.e.  $T_a > T_{\text{canopy}}$ ) flow:

$$\psi_M = \psi_H = 6 \ln(1 + \zeta)$$

$\zeta$  = atmospheric stability

$$\zeta = - \frac{0.4 g z H}{\rho c_p T_a u^{*3}} \quad (T \text{ in kelvin})$$

$$u^* = \text{friction velocity} = \frac{0.4 u(z)}{\ln \frac{z-d}{Z_M}}$$

$u^*$  after first iteration (calculate  $\zeta$  with this  $u^*$  after the first step in the iteration process)

$$= \frac{0.4 u(z)}{\ln \left( \frac{z-d}{Z_M} \right) + \psi_m}$$

$H$  = sensible heat flux =  $g_{Ha} * c_p (T_{\text{canopy}} - T_a)$

→ Calculating  $g_{Ha}$  requires knowledge of  $g_{Ha}$

→ iteration required: Start : random value for  $g_{Ha}$  (e.g. 1) → calculate  $H$  → calculate  $u^*$  (leave out  $\psi_M$  in first calculation only) → calculate  $\zeta$  → calculate  $\psi_M$  and  $\psi_H$  → calculate  $g_{Ha}$  → calculate  $H$  → calculate  $u^*$  (based on  $\psi_M$  from previous iteration) → calculate  $\psi_M$  and  $\psi_H$  → calculate  $\zeta$  → calculate  $g_{Ha}$  → etc.

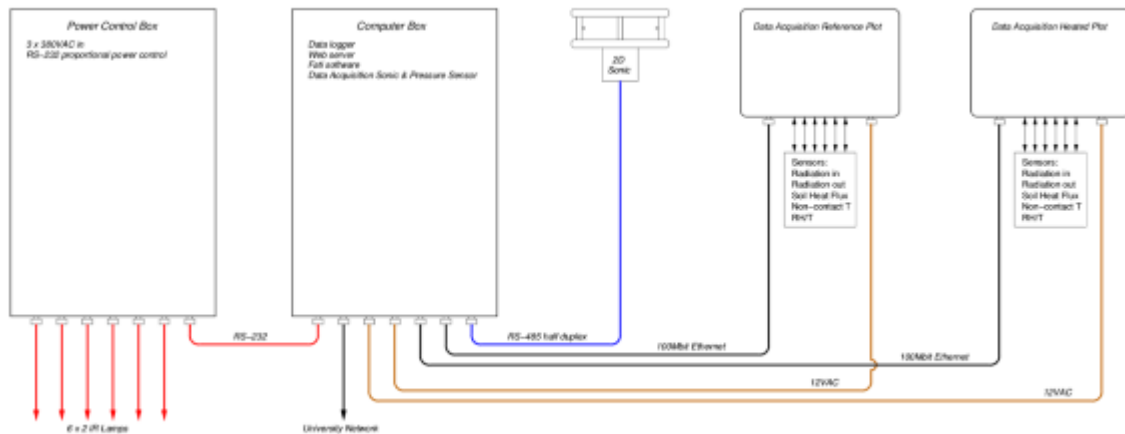


Fig. 1: Schematic of infrared heating control installed at the University of Antwerp.

### 2.3 Implementation

The technical arrangement of sensors, power supply and network is depicted in Fig. 1. After carrying out (computer) simulation runs, we did field tests at our experimental set-up on campus Drie Eiken (University of Antwerp). The results were satisfactory in that performance was as expected under most conditions (Fig. 2). The combination of cool and moist conditions with leaf temperatures below air temperatures can sometimes cause some deviation, as canopy conductance values can become

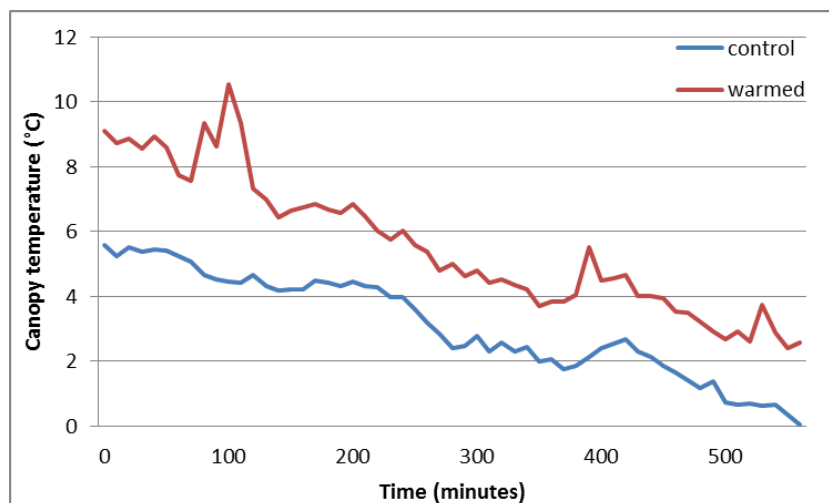


Fig. 2: Results of a test using a scenario of 3 °C warming of air temperature (the offset used in step 2, see text). The observed difference in canopy temperature between the control and warmed plots is fairly constant, with the exception of a short period around minute 100 where peculiar conditions (see text) provoked the control system to calculate a  $g_v$  that was unrealistically high (around  $35 \text{ mol m}^{-2} \text{ s}^{-1}$ ), triggering a huge demand for infrared heater radiation (fast transpiring canopy would offset a large proportion of that energy), causing a temperature spike.

erratic. By defining literature-based constraints for  $g_v$  ( $0.02 < g_v < 2.23 \text{ mol m}^{-2} \text{ s}^{-1}$ ), this issue can be remedied. Users can apply the method on any short-stature vegetation. For example, the imposed warming can be combined with withholding water in warmed plots, which should make stomatal conductance eventually diverge between the two treatments, resulting in canopy temperatures above the theoretical ones based on canopy conductance inferred from the control plot (step 2 outlined earlier). Such a temperature deviation would not be possible using a 'constant canopy temperature difference' control system.

### 3. Task T8.3: Using Computational Fluid Dynamics (CFD) to design CO<sub>2</sub> enrichment technologies

---

(contribution by CNR)

#### 3.1 The FACE technology: past, present and future

FACE (free-air CO<sub>2</sub> enrichment) has been proposed to fill a need for conducting realistic experiments to understand how plants and ecosystems will respond to the increasing ambient concentration of atmospheric carbon dioxide [CO<sub>2</sub>]. The need for such studies is apparent since nearly every life form on Earth is completely dependent on the conversion of CO<sub>2</sub> to plant matter via photosynthesis, so understanding the consequences of changes in [CO<sub>2</sub>] is a critical societal as well as scientific interest. Questions addressed by FACE include how will plants respond to the increases expected in atmospheric [CO<sub>2</sub>], how are these responses likely to feed forward into ecosystems, become limited or enhanced by ecosystem properties and how will goods and services provided to mankind by forests, crops, and natural ecosystems be altered due to these changes in atmospheric trace gases (Hendrey & Miglietta, 2006).

The pressing need to conduct plant and ecosystem fumigation experiments under realistic field conditions is widely perceived, as the limitations of chamber methods are becoming increasingly apparent. For example, open-top chambers (OTC), developed for fumigation of plants rooted in field soils, introduce many perturbations to the growth environment by altering microclimate variables such as photon flux, the ratio of diffuse to total solar irradiance, temperature, humidity, and wind stress. Typically, OTCs are about 2–4 °C warmer than ambient, light is attenuated by about 10–25 %, and wind speeds are low and steady in contrast to their great variability in the ambient environment, thus protecting the plants from physical stresses.

FACE technology permits [CO<sub>2</sub>], when averaged over minutes or longer, to be maintained stably at levels expected to prevail in the mid- to late twenty-first century.

A problem arising with the past FACE design (Hendrey et al. 1992, 1999) is that the CO<sub>2</sub>-enriched air blowing out of the vertical vent pipes has the potential to cause microclimate perturbations under very stable and calm atmospheric conditions, as on some cold nights with dew or frost formation. Under such conditions in winter, in FACE experiments with winter wheat in Arizona, FACE plots



averaged about 1 °C warmer than plots without blowers. The period of time that leaves were wetted with dew was reduced by 30% and incidence of frost on leaves was reduced. Later in the crop season, on calm nights [CO<sub>2</sub>] within ambient plots (no [CO<sub>2</sub>] treatment, no blowers) could build up to 800 ppm or even 1000 ppm due to respiration. But when blowers were operated 24 h day<sup>-1</sup>, this respiratory CO<sub>2</sub> was dissipated. Significant biological effects could conceivably occur from even these small perturbations (Pinter et al. 2000).

When seen in the perspective of innovative infrastructures, the most relevant innovations include improved and inexpensive control systems, fast-feedback PID control and more effective dilution of the fumigant. In addition, directional control was greatly improved for FACE compared to earlier systems by a microprocessor connected to a wind vane and the ability to alter directional control.

Innovative control algorithms were developed based on well-known engineering methods coupled with new ideas for improved mixing of the fumigant with ambient air. A sufficient engineering investment to assure a high degree of system reliability resulted in maintenance of [CO<sub>2</sub>] within FACE plots with much-reduced variability compared to earlier methods (Hendrey et al. 1993; Miglietta et al. 2001). The introduction of directional control, that is the release of CO<sub>2</sub> only from the upwind direction relative to the center of the FACE plot, provided a large increase in the efficiency of CO<sub>2</sub> use, hence a decrease in the cost of FACE experiments, while simultaneously maintaining acceptable control of the gas concentration.

The Institute of Biometeorology of the National Research Council (CNR) in Italy pioneered a new approach using pure CO<sub>2</sub> rather than pre-mixed air plus CO<sub>2</sub>, thus eliminating the need for blowers and leading to a substantial simplification of the equipment and hardware required to perform FACE experiments. A similar approach was independently chosen by the TNAES (Tohoku National Agricultural Station) scientists in Morioka, Japan (Okada et al. 2001). In this FACE design (Fig. 3), two or more layers of 8-m long pipes are arranged in an octagon and pure CO<sub>2</sub> is released to the atmosphere through 350 or 500 small gas jets. Mass flow is controlled by pressure within the pipes. High jet velocity creates rapid dilution with ambient air as described by Miglietta et al. (2001).



Fig. 3 A picture of the experimental FACE setup in Italy. The FACE unit was used to test and evaluate the performance of the CNR-FACE design and the verification of the new hardware that was developed and then used, including the novel PID algorithm implemented.

### 3.2 An innovative FACE design

A new FACE design has been studied using Computational Fluid Dynamics (CFD) in the frame of the EXPEER Project to create a more-or-less continuous gradient of [CO<sub>2</sub>] over an experimental area of 200 m<sup>2</sup> (GradFACE). Starting from an original unpublished idea of Prof. Kenji Kurata (Department of Biological and Environmental Engineering, University of Tokyo, Japan), this new system was initially. The CFD experiment allowed testing of a series of alternative designs, resulting in the final layout illustrated in Fig. 4. A rectangular array of laser-drilled horizontal pipes is placed over the vegetated surface, a few centimeters above the canopy height. The use of 22 automatic pressure regulators and a CO<sub>2</sub> injection control algorithm allow the release of different amounts of pure CO<sub>2</sub> from each pipe segment, depending on wind direction. In this way, more CO<sub>2</sub> is released at one end of the array and the amount of CO<sub>2</sub>, which is injected along the main direction of the array, can be decreased linearly. Model experiments indicated that specific patterns of the static pressure inside the laser-drilled pipes of the array permit maintenance of a relatively constant e[CO<sub>2</sub>] gradient over the vegetated surface, irrespective of the wind direction (Fig. 5). There may be a significant advantage in using this type of gradient design in elevated CO<sub>2</sub> studies. Tunnel experiments made in Texas (USA) created a consistent CO<sub>2</sub> concentration gradient (Polley et al. 2003) and demonstrated that non-linearities occur in plant responses as [CO<sub>2</sub>] increases.

### 3.3 Control algorithm and new hardware tests

Another significant improvement of the FACE infrastructure which was made in the frame of EXPEER, was associated to the [CO<sub>2</sub>] control algorithm (software) and the new controller (hardware) that were developed, utilized and tested in a field experiment in Italy.

Proportional-integral-derivative controller (PID controller) is a control loop feedback mechanism widely used in industrial control systems. A PID controller calculates an error value as the difference between a measured process variable and a desired setpoint. The controller attempts to minimize the error by adjusting the process through use of a manipulated variable. In the specific case of a FACE system, the PID requires an additional control on windspeed, as the pressure in the releasing valves has to be rapidly adjusted in response to sudden increase/drops of wind magnitude.

The classical PID controller algorithm involves three separate constant parameters: the proportional, the integral and derivative values, denoted P, I, and D. Each of those is transformed, in the control code into a coefficient ranging from 0 to 1 which is applied to the voltage output which controls the internal pressure of the CO<sub>2</sub>-releasing valves. P depends on the present error, I on the accumulation of past errors, and D is a prediction of future errors, based on current rate of change. The weighted sum of these three actions is used to adjust the process via a control element. A PID controller relies only on the measured process variable. By tuning the three parameters in the PID controller algorithm, the FACE controller can provide control action designed for specific process requirements. The response of the controller (its relative weight on the PID itself) set the overall responsiveness of the FACE unit, i.e. the degree to which the controller overshoots the setpoint, and the degree of system oscillation.

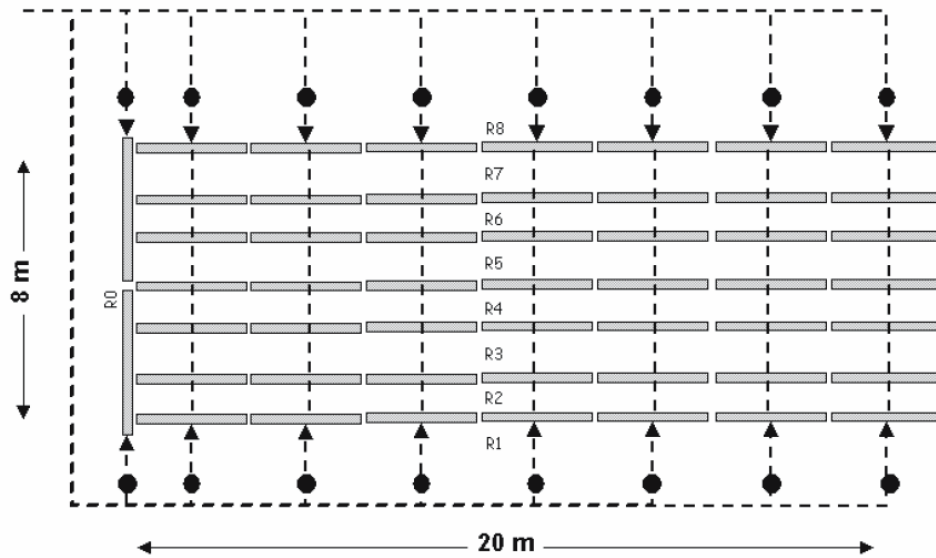


Fig. 4 GradFACE design: the pipe array is denoted by grey bars and the position of the proportional valves controlling the release of CO<sub>2</sub> from the pipe array is indicated by the black dots. Dimensions of the experimental plot used for CFD simulations are shown. As discussed in the text, the direction and intensity of wind controls the pattern of valve aperture and the amount of CO<sub>2</sub> injected over the plot.

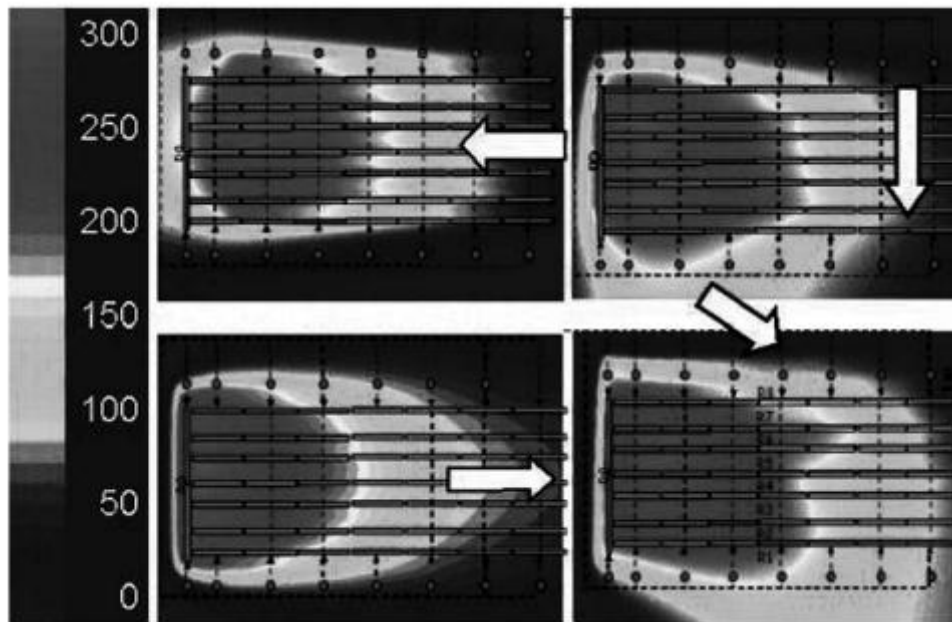


Fig. 5 Distribution of [CO<sub>2</sub>] in GradFACE (in ppm) above ambient [CO<sub>2</sub>] calculated by the CFD model at 35 cm above ground in a 15 cm tall short-grass prairie with wind blowing from four different directions (arrows). In these simulations, adjustment of valve apertures allows maintenance of a well defined elevated [CO<sub>2</sub>].

In the specific case of the CNR-FACE design the PID is implemented in a programmable logic controller as a panel-mounted digital controller (Fig. 6). Software implementations have been optimized to account for the windspeed effects and are relatively cheap and are flexible. The controller applies variable voltages within a fixed cycle time of 1 second, using running averages of 1 minute. The [CO<sub>2</sub>] sensed at the centre of the FACE ring (Fig. 7) is the process variable. The target [CO<sub>2</sub>] is called the setpoint. The difference between the [CO<sub>2</sub>] measurement and the setpoint is the error and quantifies whether the [CO<sub>2</sub>] in the center of the ring is too high or too low and how much. The obvious method is proportional control: the valve pressure is set in proportion to the current error. The rate of change of error, I, adds more or less pressure depending on how fast the error is approaching zero. Finally, integral action adds a third term, using the accumulated [CO<sub>2</sub>] error in the past to detect whether the [CO<sub>2</sub>] is settling out too low or too high and set the valve proportional to the past errors.



Fig. 6 A view of the new CNR-FACE control unit that is being operated in the FACE experimental site in Italy and is now released to other infrastructural sites in the frame of Expeer and AnaEE.

Making a change that is too large when the error is small will lead to overshoot. If the controller were to repeatedly make changes that were too large and repeatedly overshoot the target, the output would oscillate around the setpoint in either a constant, growing, or decaying sinusoid. If the amplitude of the oscillations increase with time, the system is unstable. If they decrease, the system is stable. The proportional term produces an output value that is proportional to the current error value. The proportional response can be adjusted by multiplying the error by a constant  $K_p$ , called the proportional gain constant.



Fig. 7 Field installation showing the FACE controller mounted inside a water proof box which also contains the necessary hardware for the control of the directional [CO<sub>2</sub>] release and the actuators.

### 3.4 Conclusion

FACE is a mature technology for ecological experiments that is flexible and readily adapted to a wide range of ecosystems. The recent updates and improvements are making it affordable by numerous research group and are increasing its robustness and reliability. FACE continue to offer many advantages over growth chambers or field enclosures and avoids nearly all of the artifacts associated with enclosures, canopy covers, and wind breaks. Hundreds of scientists use FACE in experiments persisting for over a decade. FACE is now applied to ecosystems ranging from the deserts to crops, bogs, conifer and deciduous forest plantations. Europe, also thanks to the activity made by CNR in the frame of the EXPEER Project has now a full leadership, worldwide. Yet, FACE technology is constantly changing and improving. FACE did not spring de novo from a single concept but was built upon a series of developments, principally improved and inexpensive micro-computer control systems and fast-feedback control algorithms. The diversity of interests of the experimenters who will contribute to FACE development led to an engineering synthesis of these technical advances with an understanding of the needs of biological field experiments and a commitment to rigorous testing from concept, to prototype, to facility. Experiments with FACE avoid changes in micro-climate observed in any type of enclosure, especially warming and altered relative humidity that impact evapotranspiration and feed forward into changes in carbon uptake.

FACE technology, despite its obvious success and contributions to science, has limitations that are often overlooked or insufficiently appreciated by users of the technology, including: the unnatural step increase in [CO<sub>2</sub>], unnatural short-term variability in e[CO<sub>2</sub>], and plot size that cannot capture some large- scale ecological processes.

A first limitation is that FACE creates a step increase in [CO<sub>2</sub>] that is some- what unrealistic and may distort early impressions of the effects of [CO<sub>2</sub>] on plants and ecosystem processes. For a crop or plantation experiment within FACE, it is obvious that the aboveground vegetation has been exposed through its entire life cycle to [CO<sub>2</sub>], but the living soil has not. Soil ecosystems acclimated to current [CO<sub>2</sub>] might take a long time to fully adjust to the increased delivery of plant products. This is one reason why it is important to continue such experiments for a long time. Is there a way around problems that might be associated with the step increase in [CO<sub>2</sub>], yet maintain a realistic manipulation experiment in the field? While one might think of ramping up [CO<sub>2</sub>] over a period of years in order to ameliorate artifacts potentially associated with a step change, that would not eliminate them unless you increment [CO<sub>2</sub>] at the same rate as our global enrichment experiment.

A second limitation is that, although variability of e[CO<sub>2</sub>] in FACE is as good as in many chambered systems, it is still highly variable, with amplitudes sometimes twice the intended treatment [CO<sub>2</sub>]. For well run FACE systems, the duration of such excursions are generally short, <60 s, and they do not significantly alter net carbon gain. Nevertheless, it is important for each type of FACE system to demonstrate convincingly the extent of the inherent variability in its ability to control e[CO<sub>2</sub>]. To assure continuous and stable operation with a high level of operational integrity, adequate staffing is needed.

The third limitation is the plot size. While the large diameter FACE plots may encompass hundreds of square meters and be sufficiently large to capture most critical ecosystem processes relating to plants and soils, they are still like an island within the surrounding ecosystem. The annular mixing zone between the points of CO<sub>2</sub> emission and the biological material to be sampled is an essential part of FACE. Experimenters are often tempted to use plants grown in this zone, but that is inappropriate as the treatment increment and condition in this zone is very irregular, some leaves receiving unacceptably high [CO<sub>2</sub>] exposures. Edge effects likely impact the entire surface of very small FACE plots.

Overall, FACE is a technology that continues to advance. New FACE concepts for producing [CO<sub>2</sub>] gradient experiments are under development with promising progress, and concepts for heated air experiments are being explored. There is a critical need to investigate the simultaneous and interacting effects of increased temperature with elevated CO<sub>2</sub> and O<sub>3</sub> concentrations. FACE experiments present us with a window into the likely future of ecosystem function in a CO<sub>2</sub>-enriched and warmer world, but are not themselves a facsimile of the future. Despite these limitations, FACE, in several different configurations, is by far the best approach to realistic, open-air field experiments yet conceived.

## 4. Task T8.4: New generation biodiversity/climate change experiments

---

(contribution by UA)

For improved climate change manipulation approaches we refer to the tested novel experimental designs for temperature and CO<sub>2</sub> control in sections 2 and 3 of this report. To improve the understanding of the role of species diversity in the functioning of multi-species plant communities, two novel experimental approaches were developed and tested. One proved unsuccessful in its practical application. The other method proved successful and was written up in a manuscript to be submitted for publication.

### 4.1 Assessing biodiversity - ecosystem functioning relationships in natural systems

#### 4.1.1 Rationale

There is a need in biodiversity research for validation of results from sown experiments with approaches closer to "natural vegetation". In sown experiments, biomass production typically increases close to linearly with increasing species richness at low richness levels, while this increase levels off at higher species richness (Hector *et al.* 1999; van Ruijven & Berendse 2005; De Boeck *et al.* 2008). Here we propose a method to test whether this diversity-productivity relation also holds in existing vegetation, by exploiting the natural micro-scale variation in species richness and biomass. The novelty of such an experiment is that, contrary to planted experiments, it tests the impact of species richness in communities that are viable without artificial human intervention such as weeding. This would make the diversity-productivity relationship more realistic. Another advantage is that long term effects are included. For example, plant-plant interactions generally grow stronger over time (van Ruijven & Berendse 2005), which would not be expressed in short-term experiments. Most importantly, this approach may avoid the bias from comparing naturally species-poor areas with naturally species-rich areas at a larger scale, where the effect of the driver behind species-richness may be detected rather than the effect of richness itself. This bias may apply less to small-scale comparisons within a single stand since the whole stand is either species-rich or poor. Nevertheless, precautions to avoid or detect bias at the smaller scales are still needed, for example, study locations should have no obvious heterogeneity (flat topography, no slope, vegetation homogeneously mixed and not gradually changing in space, no grazing since local differences due to trampling or excrements would confound the results).

#### 4.1.2 Experimental design

The study analyzed small plots in a meadow where species richness and composition are locally (scale < 1 m) different. We selected a grassland in the province of Antwerp (Belgium) that was not fertilized for 20 years and that is being mown twice a year. The measurements were conducted in August 2013. The grassland had three dominant species / functional groups (hereafter referred to as FGs): a N-fixing dicot (*Trifolium repens* L.), a non-N-fixing dicot (*Plantago lanceolata* L.) and grasses (mixture of different species). Three FGs yields seven possible combinations (A, B, C, AB, BC, AC, ABC), all of which appeared to occur locally in the meadow upon visual inspection. Having Four FGs would yield 15 possible combinations; since finding enough replicates of all possible combinations is

a requirement we assessed that three species is the limit. The sample plots were thus chosen to contain either one FG (for each of the three FGs), two FGs (all combinations), or all FGs (Fig. 8), with eight replicates per monoculture and bi- or tri-combination that were randomly distributed over the study site. The size of the plots had to be small enough to find monocultures but large enough to find all the two and three FG combinations. Given these requirements, the optimal plot size for this meadow was found to be 0.25 × 0.25 m. We aimed at keeping evenness constant (maximized) for the two and three FG combinations at 50/50 and 33/33/33 respectively. From visual inspection it was clear that sometimes a small number of individuals of other species was present in a patch; we aimed to keep this ‘contamination’ below 5 to 10 %. Another problem that arose while choosing the plot locations was that the same individual was sometimes part of a monoculture, or of a bi- or tri-FG mixture depending on where the frame of the plot was placed. Therefore, the plots were selected in a way that the borders around them represented the content of the plot. Aboveground biomass of the plots was harvested and weighed to construct the biomass-FG richness curve, similar to what is done in sown experiments. Soil samples for C, N, P and texture analysis were also taken to test the homogeneity of the field.



Fig. 8. Local monoculture, two-species mixture and three-species mixture in the sampled species-poor grassland.

#### 4.1.3 Results and conclusions

In its practical implementation, the method unfortunately proved unsuccessful. First, finding a suitable study site was problematic. Sites should not contain too many different species since, from a probabilistic point of view, the chance of finding patches with monocultures will become very small. Indeed, among the more than ten locations screened, only one (i.e. the aforementioned grassland) contained local monocultures of sufficient patch size. Moreover, monoculture patches with only one grass species were not available, so we had to aim for functional group richness instead as outlined above.

More importantly, the “contamination” by other species, which had appeared acceptable in terms of cover, proved too high in terms of biomass. We allowed 5 to 10% contamination based on plant cover, however, for three of the seven species combinations this cover-based-contamination translated into biomass largely exceeded 10% (Fig. 9). This was the case for the monocultures of *T. repens* and *P. lanceolata* and the combination of these two species. In particular, the biomass of *Trifolium repens* was so low that the individuals of other (small-stature) species below it distorted the target compositions of 100, 50/50 and 33/33/33 to a too great extent. The consequence of contamination of e.g. monocultures with other species is that they are actually mixtures. A possibility to deal with this problem could be to develop weighting factors in order to position plots on a species richness or FG scale in between monocultures and bi- or tri mixtures depending on the biomass fraction of each species. But this only works for contamination with species that are part of the three target FGs of the experiment, while “contamination” consisted also of other species. Finally, selecting the plots in a way that the borders around them represented the content of the plot, as explained



above, was not always possible. The limited distance to neighborhoods with other species combinations (e.g. N-fixers) may have confounded the results.

For these reasons, we cannot interpret the results (flat curve instead of increasing aboveground biomass with increasing local FG richness as was found in many experiments with synthesized systems, see Fig. 10). We therefore decided to abandon the method and concentrate resources on the method in the following section.

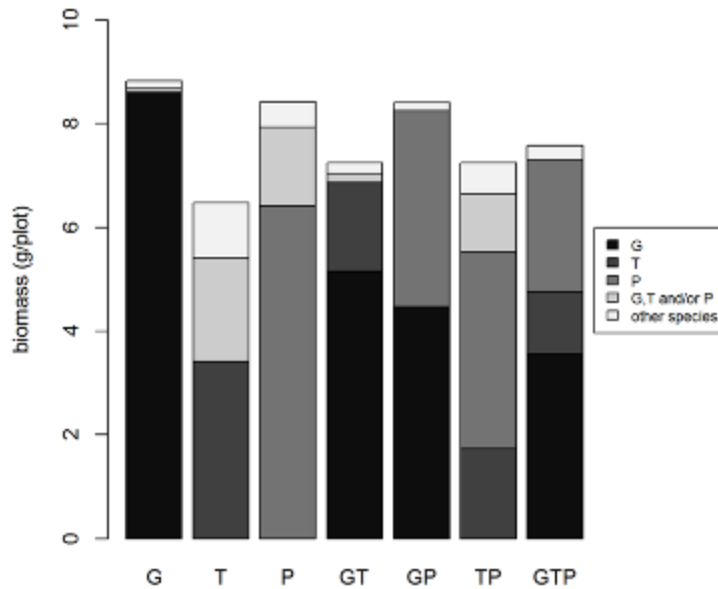


Fig. 9. Biomass per functional group combination in the grassland, as determined in 25 cm × 25 cm plots which contained either one, two or three functional groups. The species were a N-fixing dicot (*Trifolium repens* (T)), a non-N-fixing dicot (*Plantago lanceolata* (P)) and grasses (mixture of different grass species (G)).

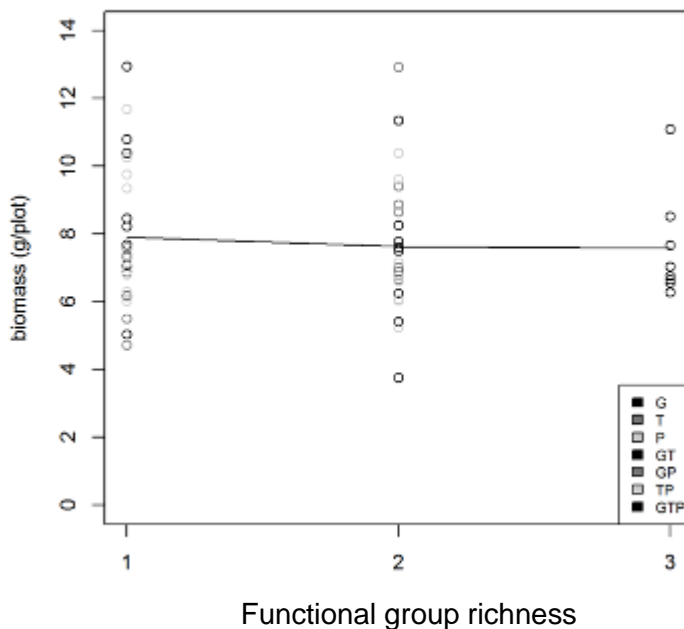


Fig. 10. Aboveground biomass in the 25 x 25 cm grassland plots, containing either monocultures, two-functional group mixtures and three functional group mixtures. The species were a N-fixing dicot (*Trifolium repens* (T)), a non-N-fixing dicot (*Plantago lanceolata* (P)) and grasses (mixture of different grass species (G)).

## 4.2 Quick method for characterizing species interactions in a plant community

### 4.2.1 Rationale

Characterizing the interactions between the species in diverse plant communities is a methodological challenge in ecology. In landscapes where the suitable habitat occurs in patches (e.g. forest remnants in a matrix of agricultural land, or oceanic islands), the interactions between the species can be studied by detecting the positive or negative spatial associations between them. To this end, the observed co-occurrence of species in the patches or on the islands is compared with an expected co-occurrence in null models that randomize the presence of the species across the patches. However, many landscapes do not host plant communities in habitat patches embedded in an unsuitable matrix, but in continuous vegetation such as grassland, heathland, forest, etc. In these cases, methods to explore interactions are cumbersome, and usually entail fully mapping the vegetation. Perhaps this is the reason why thousands of studies have made vegetation surveys, but few have focused on detecting the  $S^2$  possible interactions in communities with  $S$  species (assuming that the influence of species  $X$  on species  $Y$  can be different from the influence of  $Y$  on  $X$ , and also taking into account the intraspecific interactions  $X-X$ ,  $Y-Y$ , etc.). For example, a 20-species community would comprise the study of 400 possible interactions.

### 4.2.2 Experimental design

Here we present a simple and fast method for detecting the interactions between species in a plant community (or a community of sessile organisms in general), which we apply on a ruderal plant community as an example. The method is based on the principle that abundant species have a greater chance to be a neighbour of a target individual than rare species. The method consists of two steps: the first is to construct the rank-abundance curve, which can be done with a classical vegetation survey, while the second step consists of scoring the nearest neighbours of target individuals.

The rank-abundance curve plots the relative abundances of the species in the community, ranked from high (dominant species) to low (rare species). The relative abundance of species  $X$  is defined as the fraction of the individuals of species  $X$  relative to the total number of individuals of all the species in the community. This can be measured by laying out a sufficiently large number of (usually square) plots of suitable dimension. For the second step, a sufficiently large number of individuals of species  $X$  are randomly selected, and each time the identity of the nearest neighbour is recorded. This is repeated for all species in the community. Comparing the observed relative frequency of neighbourships of a species with what is expected based on the relative abundance of each species in the community, provides information on the nature of the interactions between the species.

The data are compiled in a single plot per species  $X$  (example in Fig. 11). In this plot, every symbol represents a species of the community. The abscissa of each symbol is the relative abundance of the species, and the ordinate is the relative frequency of that same species as neighbour of species  $X$ . Imagine that species  $A$  is the most abundant species, with a relative abundance of 30%. We then expect 30% of the neighbours of species  $X$  to be species  $A$ , provided that contacts between species  $X$  and species  $A$  are not overrepresented or underrepresented in the community. If  $B$  is the next most abundant species represented by 15% of the individuals, then we expect 15% of the neighbours of

species X to be species B, again assuming no over- or underrepresentation. The same expectation applies to all the other species neighbouring species X, such that the expected plot for species X with neighbourhood frequency as a function of relative abundance is a straight line going through the origin (0%,0%) and the point (100%, 100%). Deviations between the observed values (abundance %) and the expected values (neighbourship %) signify over- or underrepresentation of the contacts between species X and its neighbouring species (including itself, as same-species contacts are also recorded). Note that the sum of the contact frequencies (Y-axis values) is always 100%, which implies that species that have more contacts with species X compared with their relative abundance, must be compensated by other species that have less contacts with species X than anticipated based on their relative abundance. Neighbourships that are overrepresented point to facilitation, neighbourships that are underrepresented point to competition.

Separate plots are made for every species X in the community, which always contain all the species. On each of these plots, the abscissa values (i.e. the relative abundances) are the same. This is because, regardless of whether species X is a dominant species or a rare species, it is always expected to 'meet' species according to their observed relative abundances.

Data were collected in a real community to illustrate the method. A ruderal field in the province of Antwerp (Belgium) was selected which was previously a corn field. The species present were: *Trifolium pratensis* L., *Lotus corniculatis* L., *Chenopodium album* L., *Malva sylvestris* L., *Solanum nigrum* L., *Taraxacum officinale* Wigg., *Leucanthemum vulgare* Lam., *Cirsium arvense* L. (Scop.), *Achillea millefolium* L., *Lolium perenne* L., *Holcus lanatus* L., and *Conyza canadensis* (L.) Cronq (see rank-abundance curve in Fig. 12). We used a homogenous subsection of the field of 18 m long and 3.2 m wide. To assess the relative abundance of each species, 46 plots of 0.25 × 0.25 m were (regularly) distributed across the subsection. In each plot the number of individuals of each species was counted. Neighbourships were determined only for the six most abundant species (rarer species had insufficient individuals to assess the contact distribution). Per species, 91 neighbours were identified, which were likewise distributed homogeneously across the sampling area.

### 4.2.3 Results and conclusions

Data were processed for all species and the significance of the deviations between the observed and the expected associations were tested with a Chi-square test. Of the six species tested (others were too rare), only the graph for *Malva sylvestris* showed significant deviations from the 1:1 line, i.e. a combination of positive and negative associations (Fig. 12). For example, *Trifolium pratensis* occurred significantly more as neighbour of *Malva sylvestris* than expected by chance, suggesting positive interaction. Conversely, *Taraxacum officinale* occurred significantly less as neighbour of *Malva sylvestris* than expected by chance, suggesting negative interaction.

The data collection for the method was completed in three person-days, which makes the method feasible for rapid screening of possible interactions in multi-species communities.

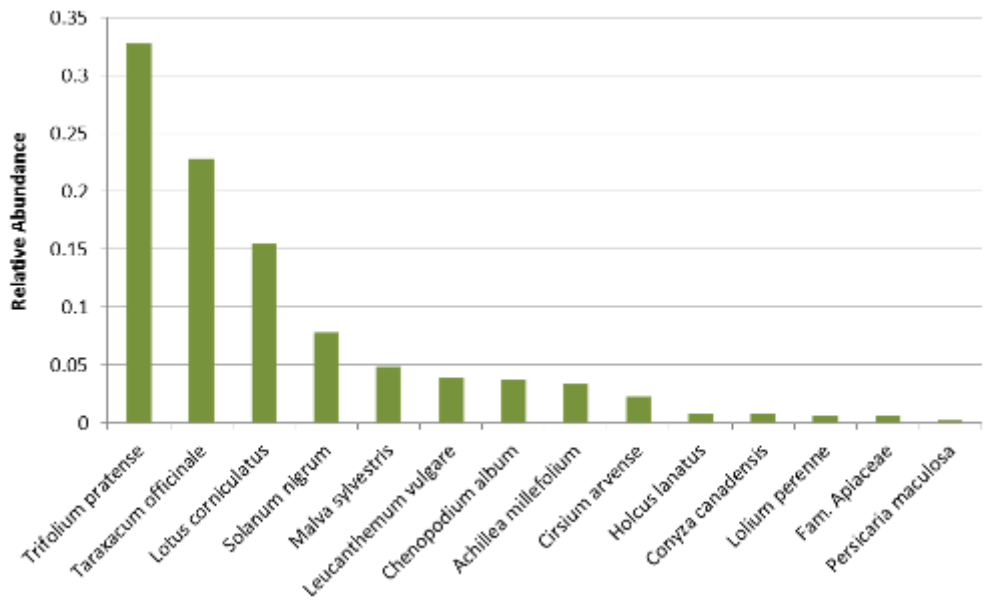


Fig. 11. Rank abundance curve of the species observed in the test experiment.

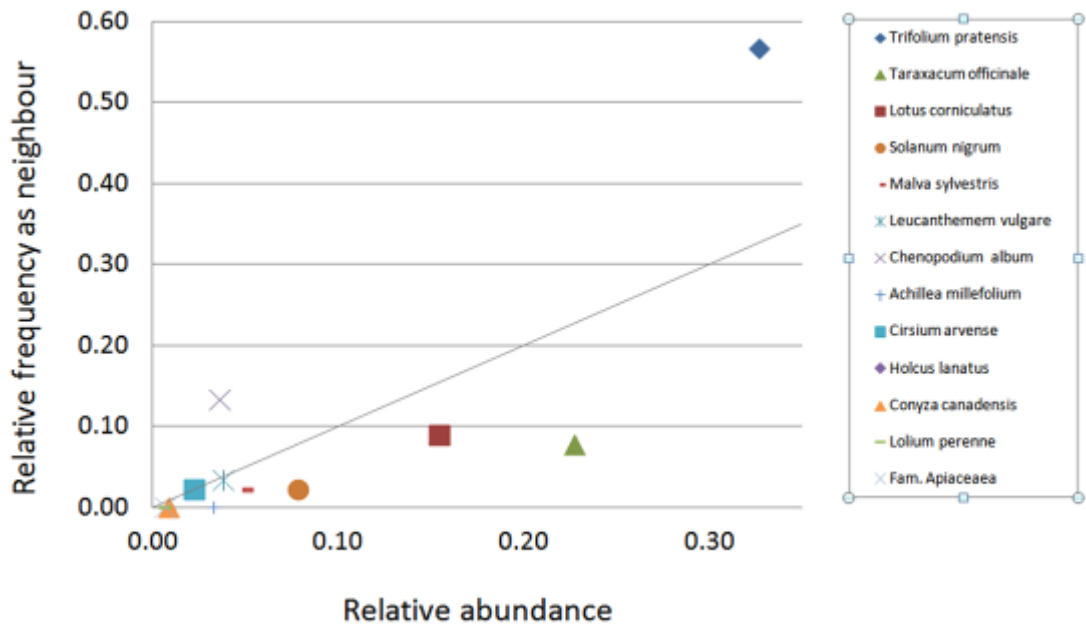


Fig. 12. Example of relationship between relative neighbourhood frequencies and relative abundances, for target species *Malva sylvestris*.

## Annex

### 1. Deliverable Check list

To be completed by Deliverable leader

	Check list	√	Comments
BEFORE	I have checked the due date and have planned completion in due time	v	Please inform project management team of any foreseen delays
	The title corresponds to the title in the DoW (Description of Work)	v	<b>The work on small-scale proxies of whole ecosystems by IMPERIAL (Task 8.3) was already finalized earlier and is included in D8.1. Test results on new types of model ecosystems by CNRS (Task 8.3) will be reported in D8.4.</b>
	The contents corresponds to the description in the DoW (Description of Work)		
	The dissemination level corresponds to that indicated in the DoW (Description of Work)	v	
	The contributors (authors) correspond to those indicated in the DoW (Description of Work)	v	
	The Table of Contents (ToC) has been validated with the WP Leader	v	Please validate the ToC with the WP leader before drafting the deliverable
	I am using the ExpeER deliverable template (title page, styles etc)	v	Can be found in the intranet
AFTER	The deliverable has been reviewed internally in my organization	v	Please ask colleagues to review the deliverable for its scientific content
	The deliverable has been reviewed by all contributors (authors)	v	Make sure all contributors have reviewed and approved the final version of the deliverable. You should leave sufficient time for this validation.
	I have done a spell check and had the English verified	v	Ask a colleague with a good level of English to review the language of the text and do a spell-check too.
	I have sent the final version to the WP Leader for approval	v	Please send the final validated draft to the Coordinator (project management team) & ExC for validation before the submission to the EC.